CHARPTER II

RELATED THEORICAL

Piezoelectricity

The word "piezoelectricity" is translated from the Greek word *piezein* which means pressure electricity. This word was discovered by Jacques Curie and Pierre Curie in 1880 [25]. Piezoelectricity is an electromechanical coupling phenomenon occurring in non-centrosymmetric crystalline materials. A piezoelectric crystal will develop an electrical charge in response to an applied mechanical stress to materials (direct effect). Conversely electrical energy can be converted into mechanical energy through the reorientation of dipoles, which rearranges the crystal lattice (converse effect). The piezoelectric effect is linear (first order), producing a strain proportional to the electric field with the displacement directionally dependent on the sign of the applied electric field. The schematic diagram of direct effect and converse effect is illustrated in Figure 1.

Electrostriction is a quadratic (second order) effect in which strain is independent of direction and proportional to the square of the electric field. This phenomenon is the electromechanical response observed in a centrosymmetric crystal, for which no polar properties exist. The elctrostrictive effect is usually very weak with strain on the order of 10^{-11} in simple oxides and 10^{-6} in perovskite oxide. However, some perovskites with high dielectric constants (indicating a high degree of polarizability) can exhibit large electrostrictive electromechanical coupling, with strains on the order of 10^{-3}. High-strain electrostrictors are the preferred materials for high precision controller actuator applications, for they have negligible hysteresis (i.e. no shift of the initial zero position) and do not require electric polling to preferentially orient dipoles or domains [26].

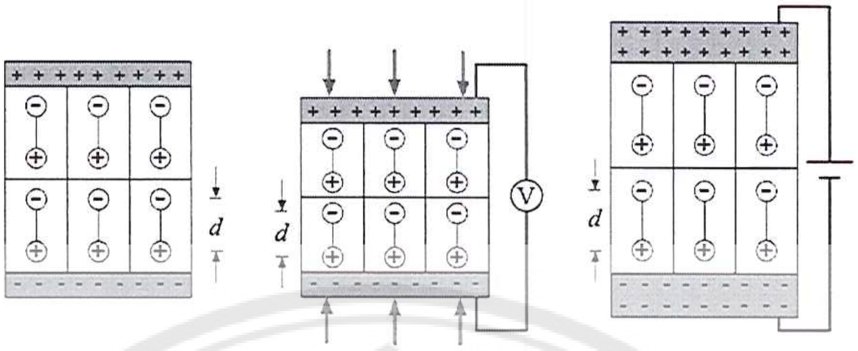

(a) (b) (c)

Figure 1 (a) Schematic illustration of electric dipoles within piezoelectric materials, (b) Compressive stresses on materials cause a voltage difference (direct effect), (c) Applied voltage causes materials deform thecrystal lattice (converse effect) [26]

Ferroelectricity

Ferroelectricity (FE) was first discovered in Rochelle salt in 1921. At that time, it was called Seignette-electricity, honoring its discoverer. For the past few decades, ferroelectric materials have received great interest because of their various uses for many applications such as high-permittivity capacitors, pyroelectric sensors, piezoelectric transducers, eletrooptic devices and PTC thermistors [27].

A crystal is ferroelectric when it possesses at least two equilibrium orientations of the spontaneous polarization in the absence of an external electric field. Its spontaneous polarization can be switched between those orientations by an applied electric field. The polar character of the orientation states should represent an absolutely stable configuration in a null field [27]. Among the 32 crystal classes, eleven of them are characterized by the existence of a center of symmetry. The remaining 21 crystal classes do not have a center of symmetry. Thus, it is possible for the 21 groups to (i) have one or more polar axes, and (ii) possess odd-rank tensor properties. The only exception is the group 432. Although it lacks a center of symmetry, it has other symmetry operations that destroy polarity. All non-centrosymmetric point groups exhibit a piezoelectric effect that is defined by a change of electric polarity under applied stress. Out of the twenty piezoelectric classes, ten possess a unique polar axis. The spontaneous polarization depends on temperature. This is called the pyroelectric effect. Ferroelectric crystals belong the pyroelectric family, which in addition has a spontaneous polarization which can be reversed by an external electric field. Among all ferroelectric materials, the most extensively studied and widely used are the perovskite crystal. A perfect perovskite structure has a general formula of ABO_3, where A represents a divalent or trivalent cation, and B is typically a tetravalent or trivalent cation. The interrelationship of piezoelectric and subgroup on the basis of symmetry is showed in Figure 2.

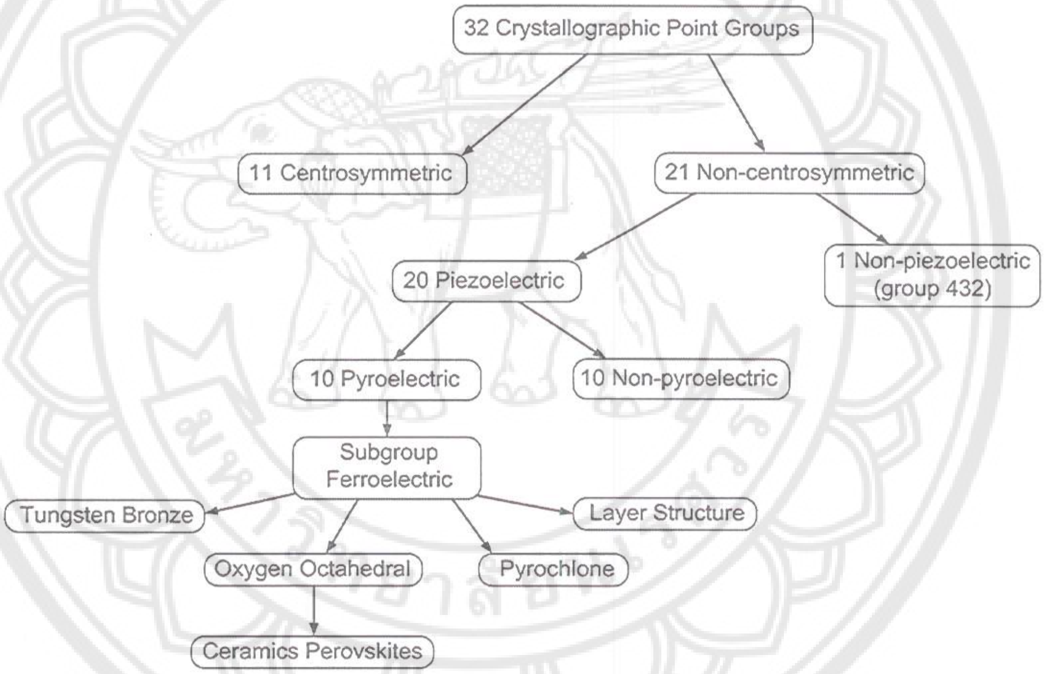

Figure 2 Interrelationship of piezoelectric and subgroup on the basis of symmetry

The origin of ferroelectricity in this family of materials can be explained by the well-known example of barium titanate ($BaTiO_3$). As shown in Figure 3, the Ba^{2+} and Ti^{4+} cations are located at A-site and B-site of the unit cell, respectively [25].

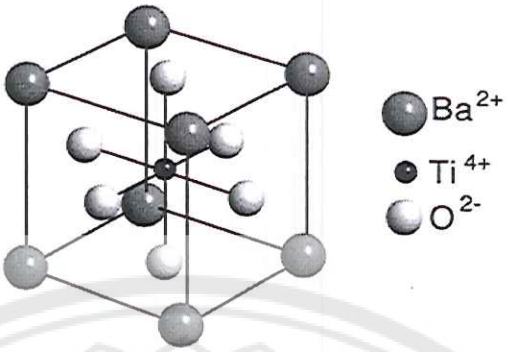

Figure 3 Ion positions in $BaTiO_3$

Typical interested properties of ferroelectric ceramics materials

1. Dielectric properties

Consider two metal parallel plates of area *A* separated by a distance *d* in vacuum (Figure 4(a)). Attaching these plates to a simple electric circuit and closing the circuit will result in a transient surge of current that rapidly decays to zero. As shown in Figure 4(b). Given that

$$Q = \int I \, dt \qquad \text{[Eq.1]}$$

The area under the *I* versus *t* curve is the total charge that has passed through the circuit and is now stored on the parallel plates.

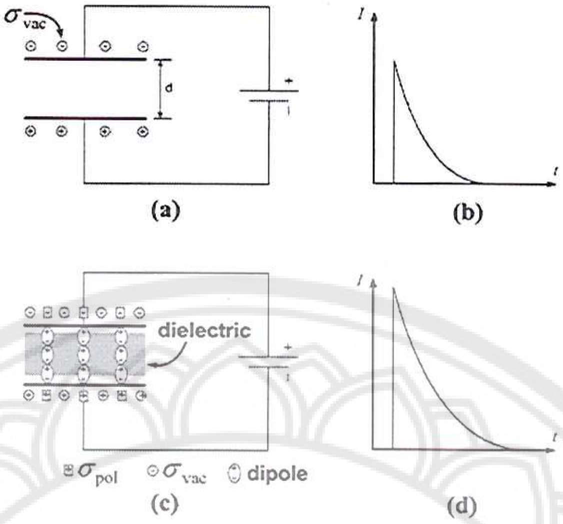

(a) (b)

(c) (d)

Figure 4 (a) Parallel-plate capacitor of area A and separation d in vacuum attached to a voltage source, (b) Closing of the circuit causes a transient surge of current to flow through the circuit, (c) Parallel-plate capacitor of area A and separation dielectric materials is placed between the plates, (d) Closing of the circuit results in a charge stored on the parallel plates of (c) circuit

Repeating the experiment at different voltages V and plotting Q versus V should yield a straight line (as shown in Figure 5). The well known relationship is

$$Q = CV \qquad \text{[Eq.2]}$$

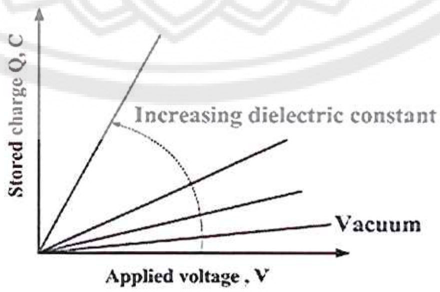

Figure 5 Functional dependence of Q on applied voltage. Slope of curve is related to the dielectric constant of the material

The slope of the Q versus V curve is the capacitance C_{vac} of the parallel plates in vacuum, given by

$$C_{\mathrm{vac}} = \frac{\varepsilon_0 A}{d} \qquad \text{[Eq.3]}$$

Where ε_0 is the permittivity of free space, which is a constant equal to $8.85 \times 10^{-12}\,\mathrm{C^2/(J \cdot m)}$.

If a dielectric which can be a gas, liquid or solid is introduced between the plates of the capacitor (Figure 4(c)), the current that flows through the external circuit and is stored on the capacitor plates will increase (Figure 4(d)). Repeating the experiment at different voltages and plotting the total charge stored on the capacitor versus the voltage applied will again result in a straight line but with a larger slope than that for vacuum (Figure 5). The capacitance of the parallel plates is modified to form

$$C = \frac{\varepsilon A}{d} \qquad \text{[Eq.4]}$$

Where ε is the dielectric constant of the material between the parallel plates. The relative permittivity or dielectric constant of a material ε_r is defined as

$$\varepsilon_r = \frac{\varepsilon}{\varepsilon_0} \qquad \text{[Eq.5]}$$

Which when combined with Eq.4 and Eq.5 gives

$$C = \frac{\varepsilon_r \varepsilon_0 A}{d} = \varepsilon_r C_{\mathrm{vac}} \qquad \text{[Eq.6]}$$

Thus ε_r is a dimensionless parameter that compares the charge-storing capacity of a material to that of vacuum.

2. Polarization

By combining of the Eq.2 and Eq.3, the σ_{vac} is the surface charge in vacuum and defined as

$$\sigma_{\mathrm{vac}} = \left[\frac{Q}{A}\right]_{\mathrm{vac}} = \frac{\varepsilon_0 V}{d} = \varepsilon_0 E \qquad \text{[Eq.7]}$$

When a dielectric is introduced between the parallel plates (Figure 4(c)), the surface charge on the parallel plates increases to

$$\left[\frac{Q}{A}\right]_{\text{dic}} = \frac{\varepsilon_0 \varepsilon_r V}{d} = \sigma_{\text{vac}} + \sigma_{\text{pol}} \qquad \text{[Eq.8]}$$

Where σ_{pol} is the excess charge per unit surface area present on the dielectric surface. The σ_{pol} is numerically equal to the polarization (P) of the dielectric.

$$P = \sigma_{\text{pol}} \qquad \text{[Eq.9]}$$

The surface charge on the parallel plates is defined as dielectric displacement (D) which when combined with Eq.7 and Eq. 9 gives

$$D = \sigma_{\text{vac}} + \sigma_{\text{pol}} = \varepsilon_0 E + P = \varepsilon \varepsilon_0 E \qquad \text{[Eq.10]}$$

Further combining Eq.7 to Eq.10, one sees that

$$P = (\varepsilon_r - 1)\varepsilon_0 E = \chi_{\text{dic}} \varepsilon_0 E \qquad \text{[Eq.11]}$$

Where $\chi_{\text{die}} = \frac{\sigma_{\text{pol}}}{\sigma_{\text{vac}}}$ and defines the dielectric susceptibility of the material.

3. Hysteresis loop

Ferroelectric materials can switch their spontaneous polarization by an applied electric field. The reversal polarization can be observed by measuring the ferroelectric hysteresis as shown in Figure 6. As an applied electric field is increased, the polarization increases rapidly and reaches a saturation polarization (P_s). Upon decreasing an electric field back to zero, polarization does not fall to zero. Some of the domains in crystal remain aligned in the positive direction; hence the crystal will show a remanent polarization (P_r). Upon reversing the direction of electric field, the polarization is removed and a net zero polarization is occurs at a coercive field (E_c). Further increases in the reverse field lead to saturation of polarization in the opposite direction.

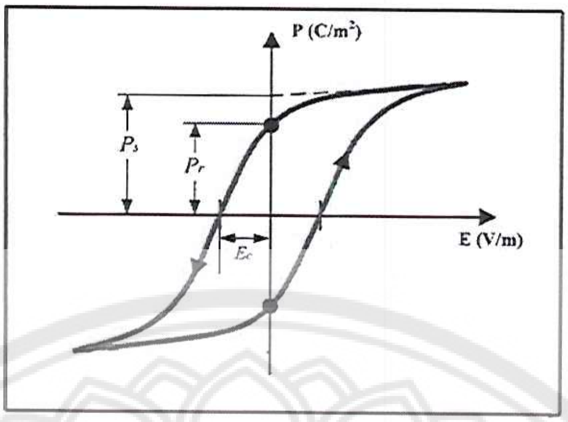

Figure 6 A typical ferroelectric hysteresis loops

4. Phase transition and Curie temperature

All ferroelectric materials have a transition temperature called the Curie temperature (T_c) [28]. At a temperature $T > T_c$ the crystal does not exhibit ferroelectricity. While $T < T_c$, the crystal shows ferroelectric characteristics. On decreasing the temperature through the Curie point, a ferroelectric crystal undergoes a phase transition from a non-ferroelectric phase to a ferroelectric phase. If there are more than one ferroelectric phases, the temperature at which the crystal transforms from one ferroelectric phase to another is called the transition temperature.

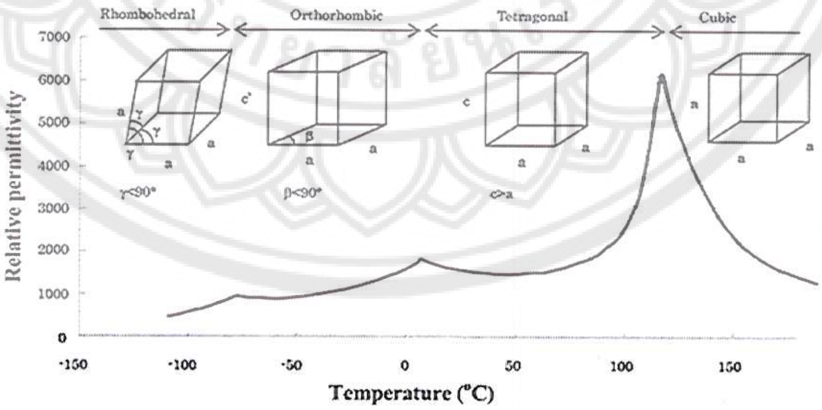

Figure 7 Variation of relative permittivity with temperature for $BaTiO_3$ [25]

Figure 7 shows the variation of the relative permittivity with temperature of $BaTiO_3$. The crystal is cooled from its paraelectric cubic phase to the ferroelectric tetragonal, orthorhombic, and rhombohedral phases, respectively. Near the Curie temperature or phase transition temperatures, thermodynamic properties including dielectric, elastic, optical, and thermal constants show an anomalous behavior. This is due to a distortion in the crystal as the phase structure changes. The temperature dependence of the dielectric constant above the Curie point ($T > T_c$) in ferroelectric crystals is performed by the Curie-Weiss law:

$$\varepsilon_r = \frac{A}{T - \theta_c} \qquad \text{[Eq.12]}$$

Where A is a constant for a given material and θ_c is a temperature near to but not identical with the Curie temperature [25].

Typical ferroelectric matrials: Barium titanate (BT)

At high temperature, barium titanate ($BaTiO_3$) is cubic structure with the ion arranged as in Figure 8(a). Below the Curie point (approximately 120°C), the structure is slightly distored to tetragonal with the *c/a* ratio of around 1.01 and is stable. The spontaneous polarization is along one of the (001) directions in the original cubic structure. Between 0°C and -90°C, the ferroelectric orthorhombic phase is stable with the polarization along one of the (110) directions in the original cubic structure. When decreasing the temperature below -90°C the phase transition from the orthorhombic to ferroelectric rhombohedral phase leads to polarization along one of the [111] cubic directions. The phase transition behavior of $BaTiO_3$ is illustrated in Figure 7.

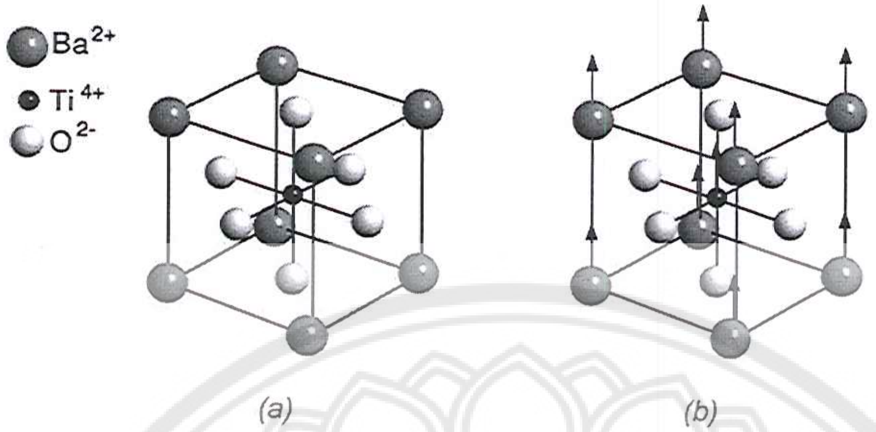

Figure 8 The crystal structures of BaTiO3 (a) Above Curie point show cubic structure, (b) Below Curie point the structure is tetragonal form with Ba^{2+} and Ti^{4+}slightly shifted relative to O^{2-}

The spontaneous polarization on cooling $BaTiO_3$ below the Curie point is due to changes in the crystal structure. As shown in Figure 8(b). Below Curie point, the structure of $BaTiO_3$ changes from a cubic to a tetragonal phase. The center of positive charges (Ba^{2+} and Ti^{4+} ions) is slightly shifted relative to negative charges (O^{2-} ion) which leads to the formation of electric dipoles. The spontaneous polarization developed is the net dipole moment produced per unit volume for the dipoles pointing in a given direction.

Typical preparation technique for ferroelectric ceramics

Solid state reaction method

The first step in the conventional method for preparing ferroelectric ceramics based on the solid state reaction method is weighing the starting materials according to the stoichiometric composition. After mixing and grinding, the mixture is usually calcined to produce the desired compound by combination reaction. Synthesis reaction of a compound is caused from the chemical reaction of raw materials, which occurs by atomic diffusion among particles at temperatures below the melting point of these raw materials. Using the diffusion laws, an equation describing the speed of solid phase reaction can be derived;

$$\left(1-(1-x)^{1/3}\right)^2=\frac{2D't}{r^2}=2Dt \qquad \text{[Eq.13]}$$

with

$$D=C\exp\left(\frac{-Q}{RT}\right) \qquad \text{[Eq.14]}$$

Where C is a constant related to the radius r of the particle, R is the gas constant, T is the absolute temperature and Q is the activation energy. This equation shows that the volume ratio x of the product increases with the increase of reaction temperatures T and reaction time t.

After calcination, the calcined powders are pressed in the mold and sintered at a higher temperature than that of the calcination. The ceramic products are densified after sintering and the grain size of the ceramic increases with increased sintering temperature.

Sol-gel method

The sol-gel process uses inorganic or metal-organic as precursors [10]. In aqueous or organic solvents, the precursors are hydrolyzed and condensed to form inorganic polymers composed of M-O-M bonds. In case of inorganic precursors, hydrolysis proceeds by the removal of a proton from an aqua ion to form a hydroxo (-OH) or oxo (=O) ligand. Condensation reactions involving the hydroxo ligands result in the formation of bridging hydroxyl (M-p(OH)-M) or oxo (M-O-M) bonds. Normally, monomeric aqueous ions are only stable at low pH and various monomeric or oligomeric anions are observed at high pH. At intermediate pH, well-defined polynuclear ions are often a stable solution. The the metal solubility is normally limited there. When it is exceeded, it results in the precipitation of oxyhydroxides or oxides.

Co-precipitation method

The concept of the co-precipitation technique is to transfer impurities to a precipitate concurrently with the deposition of some primary substances. Co-precipitation proceeds in two stages. In the first stage, the impurity is trapped either on the surface or inside the growing particles. If the growing particles have a crystal structure, then the impurity will become localized at regions of the solid phase with a perfect structure. During rapid precipitation, the growing particles will trap nonequilibrium impurities, which are usually inhomogeneously distributed through the volume of the solid phase. In the second stage, the concentration of defects within the precipitate decreases and the particles are flocculated. Impurities trapped during the first stage return either partially or completely to the medium. The concentration of impurities in the solid phase becomes equalized. The crystals acquire an equilibrium composition that depends only on the composition and temperature of the medium.

Hydrothermal synthesis method

Hydrothermal synthesis is the crystallizing of substances from high-temperature aqueous solutions at high vapor pressures. Hydrothermal synthesis can be defined as a method of synthesizing single crystals which depends upon the solubility of minerals in hot water under high pressure. The crystal growth is formed in an apparatus consisting of a steel pressure vessel. A gradient of temperature is maintained at the opposite ends of the growth chamber. The hotter end dissolves the nutrient and the cooler end causes seeds to take on additional growth.

Combustion technique

The combustion synthesis method is modified from the solid state reaction method. It is an attractive method for preparing electroceramic materials, which involves a self-sustained reaction between reaction materials and fuel (e.g., urea, glycine, citric acid). The reaction converts the initial mixture typically to a fine well-crystalline powder of desired composition [20, 21, 22]. The combustion reaction gives out the energy that can be effectively applied to the raw materials. The released energy speeds up the chemical reaction of the raw materials and also decreases the reaction temperature. Moreover, the combustion technique is simple, inexpensive and less time consuming in comparison with other methods.

Sintering process

After the powders are synthesized, the pellets should heat at high temperature to produce the desired microstructure. This stage is called in term sintering. The process of sintering consists of three stages: an initial, intermediate, and final stage [29]. For an initial stage, the green body has a low density and lacking in physical integrity. There is a small degree of adhesion between adjacent particles. After heat treatment, the local point of contact initially joins without shrinkage. This is accompanied by a smoothing of the free surface of the particles. After that, the neck formation at the contact point occurs (Figure 9). If the relative green density after the forming of the particle was 60%, the density after the initial stage would be about 70% of the theoretical density.

In an intermediate state, the significant results are the neck growth, pores forming arrays of interconnected channels and particle centers approaching one another. The high curvatures exhibited in the initial stage are assumed to have been eliminated. Densification is assumed to occur by the pore simply shrinking to reduce their radius. This stage is considered to have a relative density of 90% of the theoretical density. In the final stage, the pores are pinch off and become isolated at the grain corners. In an idealized model, the pores are assumed to shrink continuously and may disappear altogether.

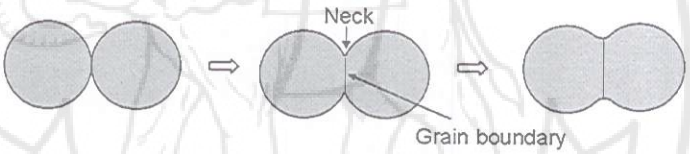

Figure 9 Schematic of two particles partly joined together on sintering process characterization techniques for ferroelectric ceramics [27]

Typical characterizations for ferroelectric ceramics

Thermal analysis (DSC and TGA)

The basis of Differential scanning calorimetry (DSC) is the measurement of heat flow which is plotted against the temperature of the furnace or the time to get a thermogram. The curve obtained in DSC is between dH/dt in mJ·s^{-1} or mcal·s^{-1} as a function of time or temperature. A typical DSC curve is shown in Figure 10. The deviation observed above the base (zero) line is called an exothermic transition and the deviation below is called endothermic transition. The area under the peak is directly proportional to the heat evolved or absorbed by the reaction, and the height of the curve is directly proportional to the rate of reaction

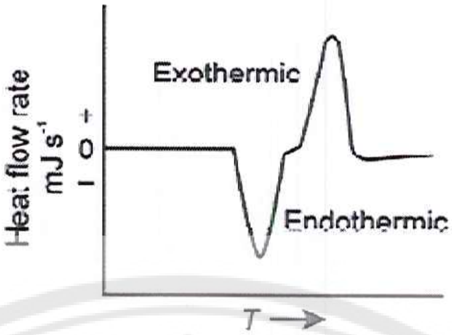

Figure 10 A typical DSC curve [29]

The block diagram of a DSC instrument as shown in Figure 11, essentially works on the temperature control of two similar specimen holder assemblies. The left half of the block diagram represents the circuit for differential temperature control while the right hand side represents average temperature control. In the average temperature control circuit, the temperature of the sample and reference are measured and averaged and the heat output of the average heater is automatically adjusted so that the average temperature of the sample and reference increases at a linear rate. The differential temperature control circuit monitors the difference in temperature between the sample and reference and automatically adjusts the power to either the reference or sample chambers to keep the temperatures equal. For getting a thermogram, the temperature of the sample is put on the *x*-axis and the difference in power supplied to the two differential heaters is displayed on the *y*-axis.

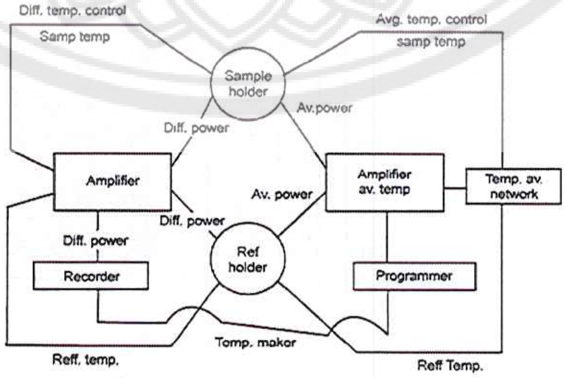

Figure 11 Block diagram of a DSC instrument [29]

Thermogravimetric analysis (TGA) is an analytical technique used to determine a material's thermal stability and its fraction of volatile components by monitoring the weight change that occurs as a specimen is heated. The measurement is normally carried out in air or in an inert atmosphere, such as Helium or Argon, and the weight is recorded as a function of increasing temperature. Sometimes, the measurement is performed in a lean oxygen atmosphere (1 to 5% O_2 in N_2 or He) to slow down oxidation. In addition to weight changes, some instruments also record the temperature difference between the specimen and one or more reference pans (differential thermal analysis, or DTA) or the heat flow into the specimen pan compared to that of the reference pan (differential scanning calorimetry, or DSC). The latter can be used to monitor the energy released or absorbed via chemical reactions during the heating process.

X-ray diffraction (XRD)

In X-ray diffraction, a collimated of mono-chromatic X rays between 0.5 – 2Å wavelength which strike a sample and are diffracted by the crystal planes present Bragg's law.

$$\lambda = 2d\sin\theta \qquad \text{[Eq.15]}$$

Bragg's law relates to the spacing between planes, *d*, to the diffraction angle, 2θ, which is scanned to pick up diffraction from the different crystal planes present. The azimuthal orientation of the diffraction beams also reveals the crystalline orientation. Distortions or broadening of the diffraction beams carry information on crystal strain and grain size. The schematic illustration of XRD analysis is illustrated in Figure 12.

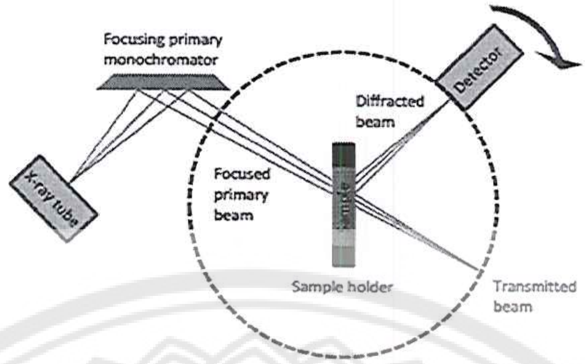

Figure 12 Schematic illustration of the diffractometer method of crystal analysis

Scanning electron microscope (SEM)

Scanning electron microscopy (SEM) is one of the most versatile and well known analytical techniques. Compared to a conventional optical microscope, an electron microscope offers advantages including high magnification, large depth of focus, great resolution and ease of sample preparation and observation. Electrons generated from an electron gun enter a surface of a sample and generate many low energy secondary electrons. The intensity of these secondary electrons is governed by the surface topography of the sample. An image of the sample surface is therefore constructed by measuring secondary electron intensity as a function of the position of the scanning primary electron beam. In addition to secondary electron imaging, backscattered electron imaging and Energy Dispersive X-ray (EDX) Analysis are also useful tools widely used for chemical analysis. The intensity of backscattered electrons generated by electron bombardment can be correlated to the atomic number of the element within the sampling volume. Hence, qualitative elemental information can be revealed. The characteristic X-rays emitted from the sample serve as fingerprints and give elemental information of the samples including semi-quantitative analysis, quantitative analysis, line profiling and spatial distribution of elements. A schematic diagram of the basic design of a SEM instrument is shown in Figure 13.

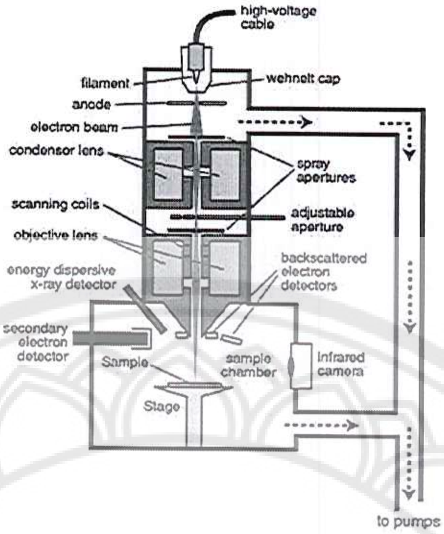

Figure 13 Schematic diagram of the basic design of a SEM [29]

Transmission electron microscope (TEM)

Figure 14 shows a schematic outline of a TEM. A TEM contains four parts: electron source, electromagnetic lens system, sample holder, and imaging system.

TEM works like a slide projector. A projector shines a beam of light which transmits through the slide. The patterns painted on the slide only allow certain parts of the light beam to pass through. Thus the transmitted beam replicates the patterns on the slide, forming an enlarged image of the slide when falling on the screen.

TEM works the same way except that they shine a beam of electrons (like the light in a slide projector) through the specimen (like a slide). However, in TEM, the transmission of the electron beam is highly dependent on the properties of the material being examined. Such properties include density, composition, etc. For example, porous material will allow more electrons to pass through while dense material will allow less. As a result, a specimen with a non-uniform density can be examined by this technique.

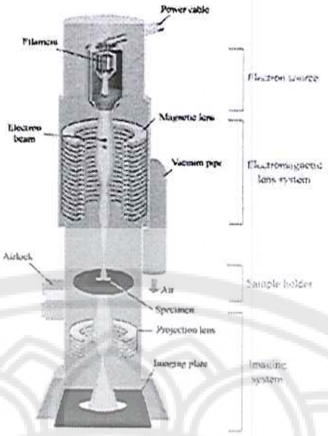

Figure 14 The schematic outline of a TEM [29]

Dielectric measurement

Parallel plate capacitor system uses a parallel plate capacitor as a sample holder, with the material under the test sandwiched between. This method requires an impedance analyzer or LCR meter. The measurements are at low frequencies, typically below 1 GHz. The material is stimulated by an AC source and the actual voltage across the material is monitored. The material test parameters are derived by knowing the dimensions of the material and by measuring its capacitance and dissipation factor. After putting a sample into a sample holder, a capacitor is formed. The parallel plate method involves sandwiching a thin sheet of material between two electrodes to form a capacitor. The measured capacitance is then used to calculate permittivity. The schematic diagram for this technique is shown in Figure 15.

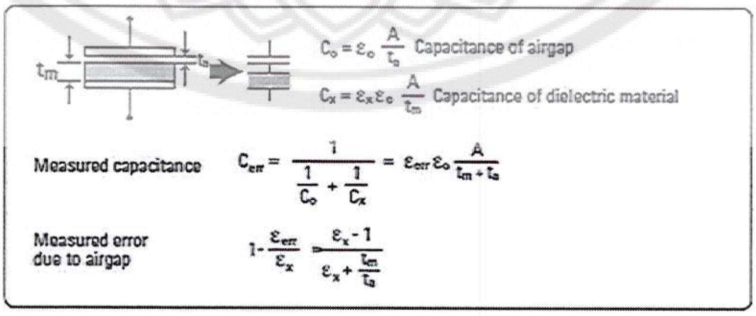

$C_o = \varepsilon_o \frac{A}{t_a}$ Capacitance of airgap

$C_x = \varepsilon_x \varepsilon_o \frac{A}{t_m}$ Capacitance of dielectric material

Measured capacitance $C_{err} = \dfrac{1}{\dfrac{1}{C_o} + \dfrac{1}{C_x}} = \varepsilon_{err} \varepsilon_o \dfrac{A}{t_m + t_a}$

Measured error due to airgap $1 - \dfrac{\varepsilon_{err}}{\varepsilon_x} = \dfrac{\varepsilon_x - 1}{\varepsilon_x + \dfrac{t_m}{t_a}}$

Figure 15 Diagram for dielectric measurement (parallel plate method) [29]

Ferroelectric measurement

A *P-E* loop for a device is a plot of the charge or polarization developed, against the electric field applied to that device (*E*) at a given frequency.

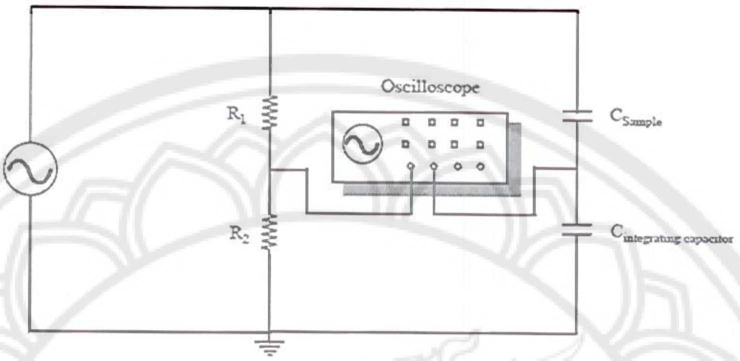

Figure 16 Schematic of a circuit for *P-E* measurement [29]

A schematic of the experimental setup is shown in Figure 16. Here the field applied across the sample is attenuated by a resistive divider, and the current is integrated into charge by virtue of a large capacitor in series with the sample. Both these voltages are then fed into the X and Y axes of an oscilloscope to generate the *P-E* loop. The applied voltage was usually a sinusoid at mains frequency as this was the simplest method to generate the required voltage and current.